Dynamic Seals Behaviour under Effect of Radial Vibration

M. SILVESTRI
Università degli Studi di Parma, Italy

E. PRATI, A. TASORA
Università degli Studi di Parma, Italy

SUMMARY
This paper presents the results of experimental and numerical tests on the behaviour of radial lip seals in order to characterize a model of the effects of vibrations and working temperature.
Starting validation of the numerical analysis, performed with the Finite Element Method, is obtained measuring the frequency response function (FRF) by using different excitation signals.
Seal's lip displacement near the dynamic clearance is measured with a strain gauge transducer in actual operating conditions. Results suggest a relationship between displacements and leakages.

1 INTRODUCTION

Radial lip seals for rotating shafts are largely used both to prevent oil leakage and to avoid dust admission. They present simplicity of maintenance and installation and have low friction torque, wear and heating with respect to other contact type seals.

Lip seals consist of an elastomer ring equipped with a strenghtening metallic insert. The ring ends, at shaft interface, with a lip. A garter spring stiffens the lip and assures a better uniformity degree of the bearing pressure between seal and shaft on varying working conditions.

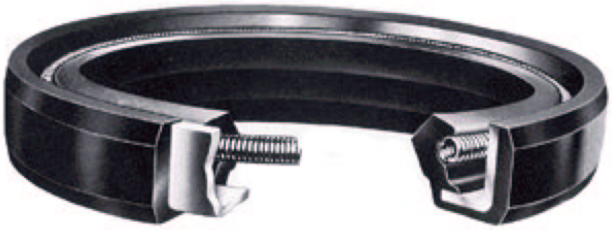

Fig. 1: A radial lip seal.

Investigations on the sealing and lubrication of radial lip seals have a long tradition, begun indentifying [1] a possible working principle. In spite of this, the complexity of the phenomena, involving different disciplines as hydrodynamics, materials science and tribology, still does not allow to develop a complete and satisfactory model.

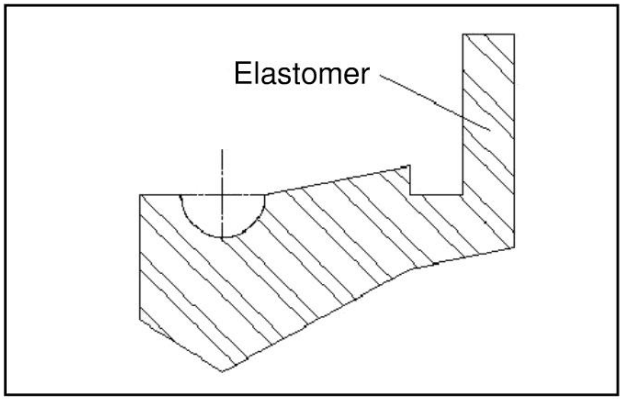

Fig. 2: Simplified section for FEM analysis.

Explanations are mainly based on micro-ondulations on the lip surface [2], [3], influence of temperature [4] and visco-elastohydrodinamic lubrication [5], [6], [7], but do not completely justify experimental results that show several stages of the leakage rate at different shaft rotating speed.

At low rotating speed, the flow increases proportionally with the speed; increasing the speed, the flow reaches a maximum which depends on the dynamic eccentricity; at greater shaft speed, the flow decreases up to a minimum; further speed increments cause flow leakage increasing

over again.

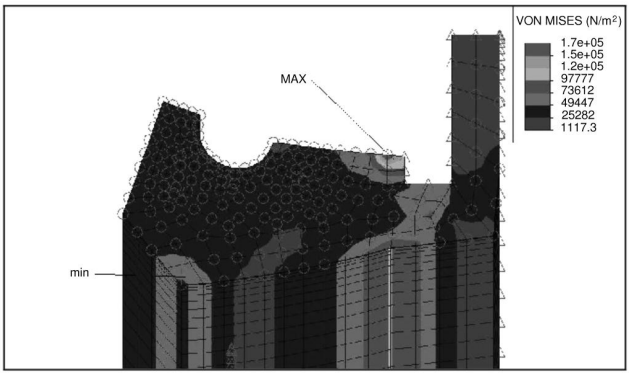

Fig. 3: Von Mises stress in a section (static analysis).

However, experimental tests gained sufficient knowledge about the working parameters that characterize the behaviour of the seals:

speed: motor rotating speed determines the frequency of the seal stress;

operating cycle: the influence of the operating cycle has already been studied [8], [9]. After first cycles of test, seal performances considerably worse, then reach steady conditions;

temperature: the temperature affects both viscoelastic properties of the rubber and lubricant viscosity;

assembly interference: difference between shaft and internal lip diameters. This parameter, fixed by the manufacturer, is fundamental for assuring the correct bearing pressure and, by consequence, the proper working of the seal;

static eccentricity: the distance between the center of the internal edge of the lip and the shaft rotation center;

dynamic eccentricity: the distance between the geometric center of the shaft section and the rotation center;

The sum of the effects produced by the eccentricities determines the entity and the distribution along the circumference of the seal stress.

In point of fact, dynamic eccentricity causes a radial oscillation of the lip points touching the shaft, while the static eccentricity modify the pressure values lenghtwise the circumference, showing a preferential zone (where the pressure is lower) for the clearance.

In order to reach a better synthesis of the tests results and the theoretical studies, we procedeed with experimental and numerical tests aimed at the investigation of effects caused by temperature and vibrations due to eccentricities, in actual working conditions.

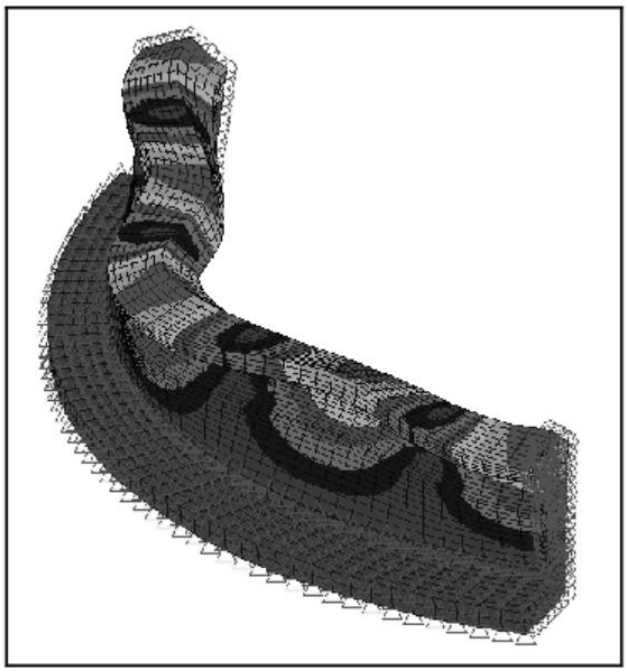

Fig. 4: Vibration mode at 420 Hz.

2 VIBRATIONS INFLUENCE

A first approach to the modeling of the studied radial seal has been turned to create a model suitable for the Finite Elements Method.

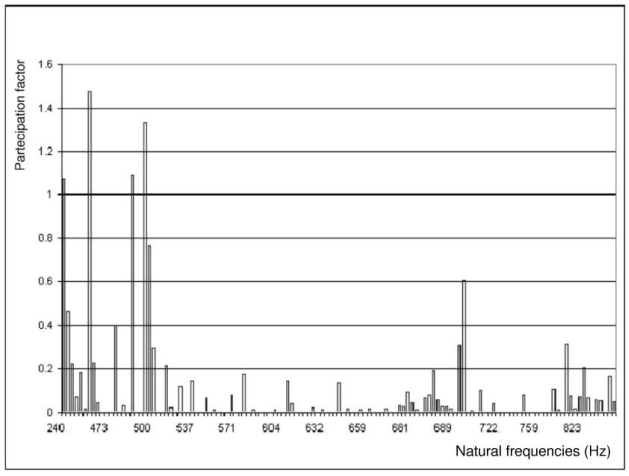

Fig. 5: Partecipation factor of natural frequencies.

Therefore an analysis of the interference seal-shaft has been performed in order to obtain elastomer stress and strain conditions. This allowed to implement the modal analysis. Figure 3 shows the Von Mises stress in a section of the seal.

The geometric modeling has been make up by a solid of rotation obtained from a simplified section. Figure

2 shows the choosen solution, which has the merit to restrict the analysis to the most stressed part of the seal (the lip). This model takes into account the studies [10], [11] and [12].

The viscoelastic behaviour of the elastomer NBR 70 is simulated in two ways: the static analysis of the interference adopts a non-linear Mooney-Rivlin model with constants $C_1 = 2,746\ MPa$, $C_2 = 4,597\ MPa$ and density $\rho = 1460\ kg/m^3$. These values are taken from [11].

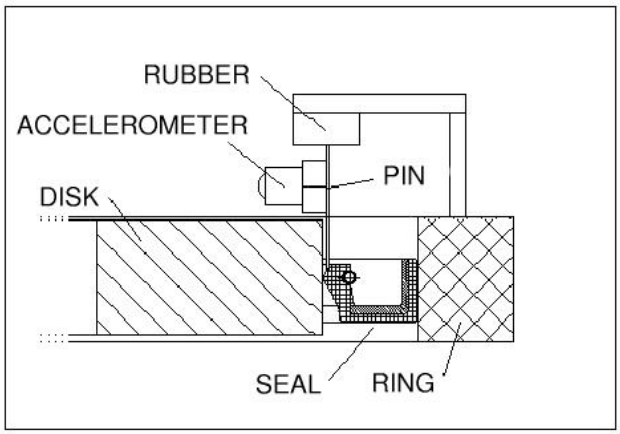

Fig. 6: Accelerometer for shaker tests.

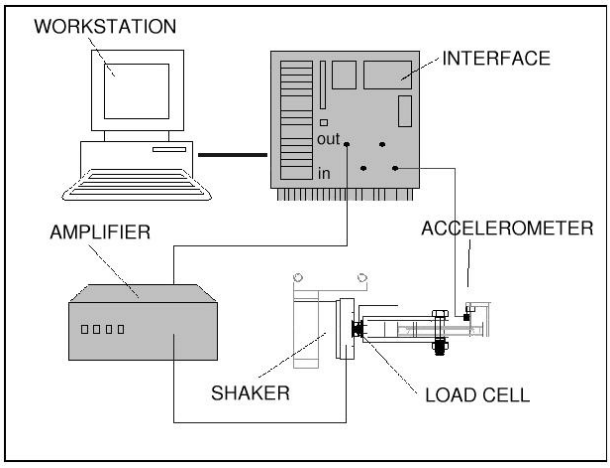

Fig. 7: Acquiring instruments for shaker tests.

The dynamic analysis would require a viscoelastic model defined as a function of the frequency. Nevertheless, the viscoelastic theory [13] allows to regard the viscoelastic materials behaviour as elastic ones, with instantaneous modulus $E_0 = (C_1 + C_2)/6$, under the following conditions: if the viscoelstic relaxation modulus reaches the asymptotic value E_1 and if $\tan\delta$ is lower than the 15% of maximum value. These are satisfied at frequencies higher than about 150 Hz.

Boundary conditions includes contacts between the seal

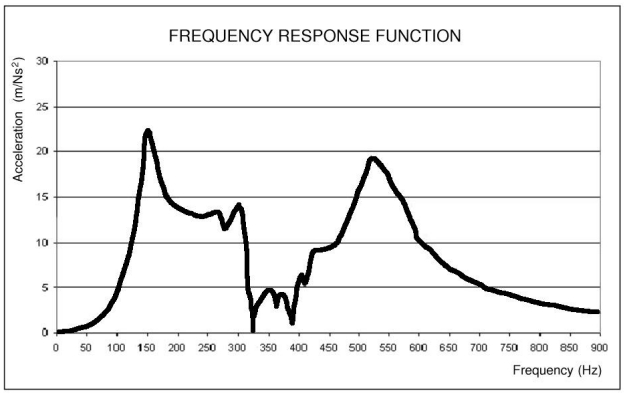

Fig. 8: FRF measured with Burst Random excitation.

surface and the metallic ring, a garter spring with $k = 0,00437\ N/mm$ [14] and the axisymmetric conditions that allow to restrict calculations to a $90°$ arc.

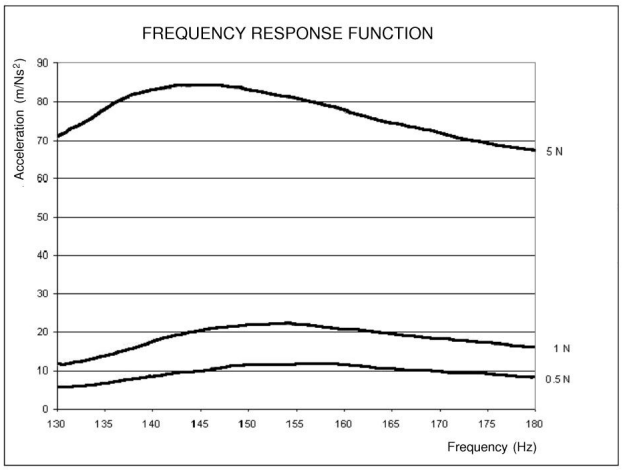

Fig. 9: FRF measured with Step Sine excitation (130-180 Hz).

Furthermore, a rigid cylindrical body with diameter $70\ mm$ simulates the shaft interference.

The analysis, performed between 0 and $1000\ Hz$, shows lots of vibration modes, starting from the natural frequency of $240\ Hz$. Figure 4 shows the mode corresponding to the frequency of $420\ Hz$.

A more significant result is given by the *partecipation factor* that the software ABAQUS uses to indicate how much the vibration modes contribute to the displacement of the lip. As figure 5 shows, the natural frequencies in ranges $250-550\ Hz$ and $700-820\ Hz$ mostly upset the seal.

The founded frequencies are fairly far from the working speed of these seals, so the results could not be experimentally validated in working conditions.

Moreover, a FRF (Frequency Response Function) analysis, that seems to be the most significant validation

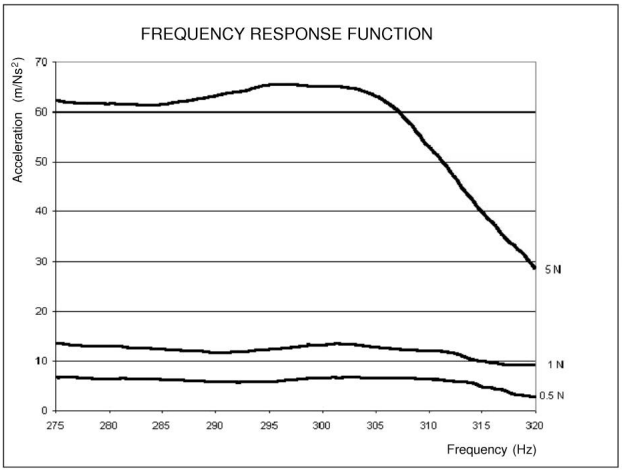

Fig. 10: FRF measured with Step Sine excitation (275-320 Hz).

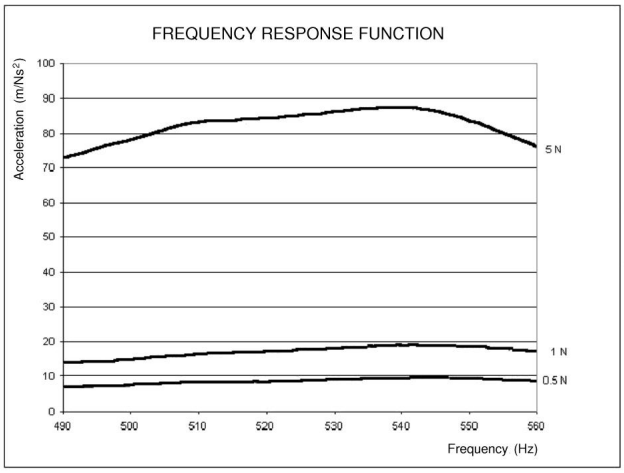

Fig. 11: FRF measured with Step Sine excitation (490-560 Hz).

for the natural frequency calculus, needs to be executed with a special apparatus which allows to sollecitate the seal by mean of a shaker.

Thus, a special testing apparatus has been built up exciting in fixed direction. The used specimen is a nitrile elastomer (NBR) with hardness 70 Shore A and dimensions $70 \times 100 \times 10\ mm$.

The experimental apparatus is made up by:

- a steel ring that simulates the seal housing, with diameter 100 mm;
- an aluminium disk that simulates the shaft, with diameter 70 mm;
- an aluminium fork that links the shaker to the disk;
- a shaker Bruel & Kjaer 4810;
- a load cell Bruel & Kjaer 8200;
- an accelerometer Bruel & Kjaer 4344;
- an amplifier OSD 1500;
- an interface Difa Scadas Q Bundle SC 206;
- a workstation HP Visualize 3000 with software LMS;

Moreover, as accelerometer dimensions do not allow to secure it directy on the lip, a steel pin with diameter 0.5 mm has been inserted in the lip and bounded at the other end with a rubber holder that allows rotating. The accellerometer is fixed to the pin as displayed in figure 6.

Figure 7 outlines the control and measure system.

Firstly tests have been performed with *Burst Random* excitation in frequency range 0-900 Hz. The result (figure 8) points out three main resonance ranges, at 130-180 Hz, 275-320 Hz and 490-560 Hz with corresponding peaks at 150, 300 and 530 Hz.

Afterwards, these resonance peaks have been investigated with *Step Sine* excitation tests, progressively increasing the applied force.

Experiments with 0,5 N, 1 N and 5 N force level show a significant nonlinearity of softening type and an amplitude increasing with the force. Figures 9, 10 and 11 summarize these results.

Experimental evidences are consistent with FEM analysis results, particulary at high frequencies. This merely confirm that the implemented elastic model has an application field limited to elevated frequencies.

3 TEMPERATURE INFLUENCE

For the purpose of achieve informations on the temperature influence, another test rig has been made, reproducing the true seal lip operating conditions: variable direction of the stress, presence of lubricant, lip wear and working temperature, that influence both the viscosity of the lubricant and viscoelastic behaviour of the rubber.

Studies of the temperature influence have been performed measuring the Frequency Response Function [15] in tests without lubrication. Other investigations concerning the leakage rate have been handled under varying temperature conditions.

Instead this work is turned to the vibrating motion of the lip at working temperature and with the presence of oil.

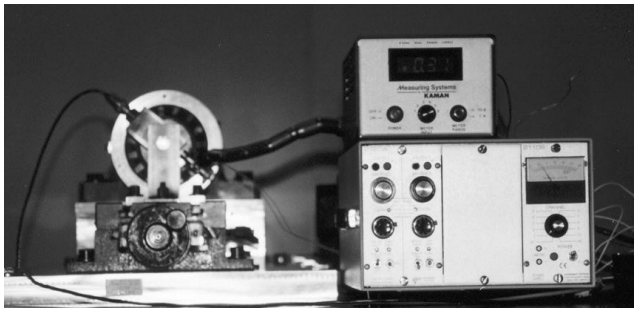

Fig. 12: Test rig.

3.1 Test rig

Test rig includes a rotating shaft machine, measuring and acquiring instruments and a strain gauges transducer built up following the concept proposed by [16].

More in details, the shaft is moved by a direct current electrical motor through a cogged belt transmission. The speed is manually controlled and can vary continuously in the 300-8000 rpm range (at the output shaft).

At the end, the shaft has a disk of circular profile which is in contact with the test seal. The dynamic eccentricity of this disk can be set to any value comprised between 0 and 0.52 mm by mean of a conical coupling. The disk is polished and has a surface roughness $R_a = 0.188\,\mu m$, as measured by using a profilometer. The position of the fixed seal housing can also be adjusted, giving the desired static eccentricity.

A fiber optics lamp lights the seal from the inside of the housing, allowing to directly verify, when the measures point out a clearance, the presence of a gap between the lip and the disk.

The temperature of the sealing lip is monitored in three different points by using thermo-couples.

As figure 14 shows, close to the disk profile is mounted a inductive sensor that collects the disk motion and hence the radial displacement imposed on the lip. The transducer depicted in figure 13 is inserted in the lip, in the zone corresponding to the maximum eccentricity.

In details, the transducer is made up by two brass cantilever located at right angles to each other, of dimensions $25 \times 12\ mm$. On each cantilever are glued two strain gauges, one for each side. At the end of the brass plate there is a steel needle with diameter $0,5\,mm$.

Seeing figure 12 can be noted that the inductive sensor and the cantilevers transducer are mounted with a phase difference of $180°$, as the two signals may easily superimposed (inverting one of them) in order to point out when actually the clearance does happen.

The apparatus also includes a signal conditioning amplifier Instrument Division 2120A for the strain gauges, a Kaman measuring systems P3500 for the inductive sensor and a National Instruments PCI-MIO-16E board that collects both the signals.

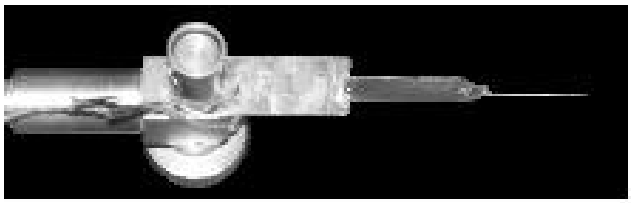

Fig. 13: The cantilever transducer.

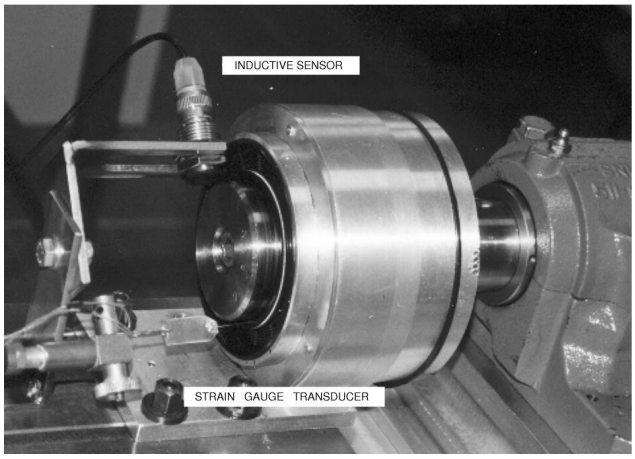

Fig. 14: The sensors assembly.

3.2 Experimental results

It is known [7] that working cycles have a great influence on the seal behaviour. In order to reach seal steady state, five working cycle of one hour at $1000\ rpm$ have been done.

Then, data have been collected varying the shaft speed between 500 and $6000\ rpm$ with steps of $100\ rpm$. Sampling rate vary from 1000 to $6000\ Hz$.

It has to be noted that also at maximum shaft speed the excitation frequency is still lower than the natural frequency of the cantilever sensor.

Static and dynamic eccentricity are, respectively: $e_s = 0,2\ mm$, $e_d = 0,35\ mm$.

Collected data clearly point out the behaviour of the lip zone involved in the clearance, as results from the graphs.

Figure 15 shows that at low speed (in this test until $1600\ rpm$) lip motion follows the radial displacement without straying from the shaft profile.

Figure 16 graph, concerning motion at $1800\ rpm$, highlights that lip motion partially leaves the shaft, generating a clearance betwen shaft and seal lip. Increasing speed the contact renewal is gathered. Graph

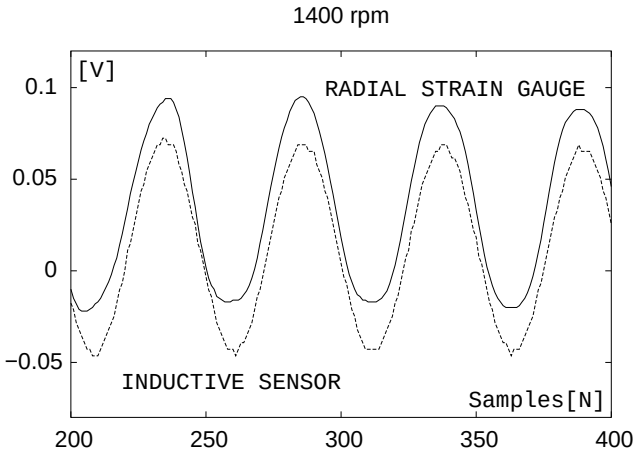

Fig. 15: Lip and shaft profile radial displacements, sample rate 1200 Hz.

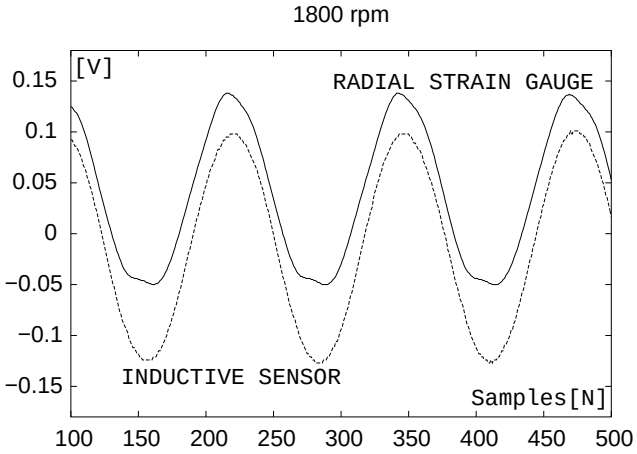

Fig. 16: Lip and shaft profile radial displacements, sample rate 3800 Hz.

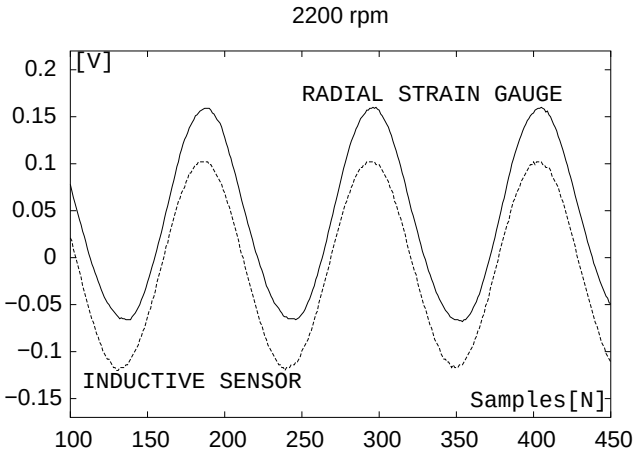

Fig. 17: Lip and shaft profile radial displacements, sample rate 4000 Hz.

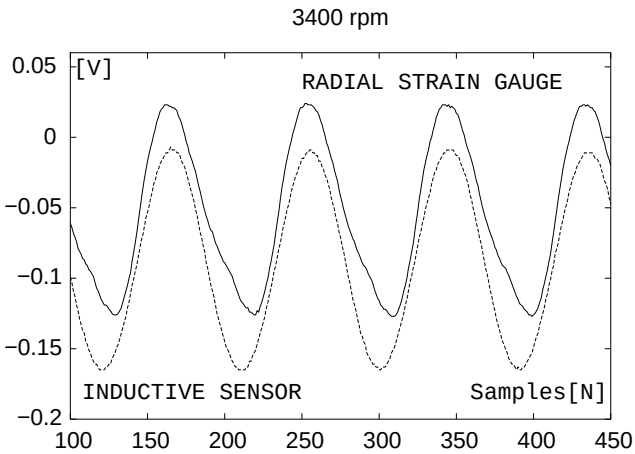

Fig. 18: Lip and shaft profile radial displacements, sample rate 5000 Hz.

of figure 17, taken at $2200\ rpm$, is meaningful about the contact resumption.

Finally, higher speeds still cause increasing lip detachments, as can be noticed in figure 18, that shows data collected at $5100\ rpm$.

This behaviour reoccurs in every test executed and corresponds accurately to leakage rates studied from [8], [9], [7].

Figures 19 and 20 show the hysteresis loop of the lip motion caused by the phase displacement between radial and tangential displacement. In particular, in case of lip detachment, a part of the hysteresis ellipse degenerates into a straight line and the overall loop area decreases.

4 CONCLUSIONS

Experimental evidences show that, at high frequencies, dynamic seals behaviour can be well approximated by a non-linear Mooney-Rivlin model.

Hence, the implemented model should be a good starting point for simulating the radial seal at working conditions and with the measured displacements of the lip in the clearance zone.

Collecting both radial and tangential lip displacement allows to quantitatively know the motion of the seal at shaft interface during the lubricant leakage.

These measures, obtained with a custom strain gauges transducer, seem to offer useful informations because of the agreement with expected leakage rate.

5 ACKNOWLEDGEMENTS

This research was supported by the grant of the Università degli Studi di Parma.

The authors acknowledge the useful help of Ing. Riccardo Longhi in the experimental tests.

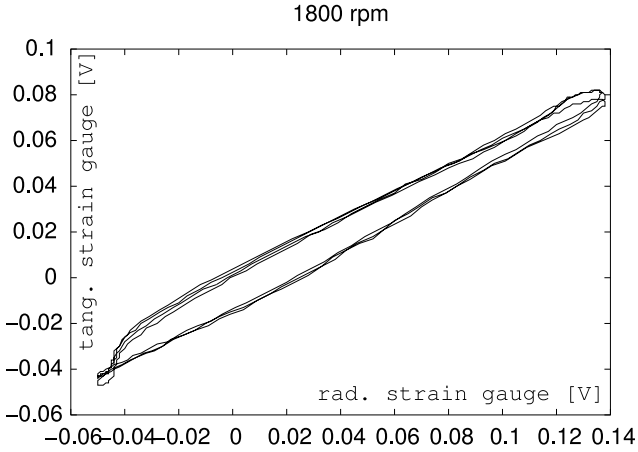

Fig. 19: Hysteresis loop in case of clearance.

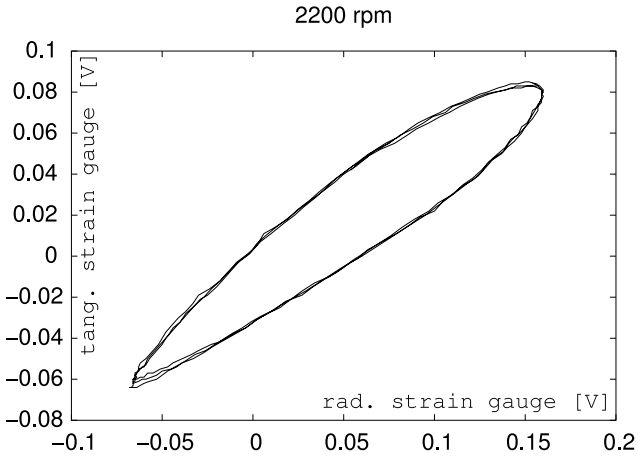

Fig. 20: Hysteresis loop in case of sealing.

REFERENCES

[1] Jagger E. T., *Study of the Lubrication of Synthetic Rubber Rotary Shaft Seals*, Proceedings of the Conference on Lubrication and Wear, I.Mech.E., pp. 409-415, 1957.

[2] Müller, H.K., *Concepts of sealing Mechanism of Rubber Lip Type Rotary Shaft Seals*, Proceedings of the 11^{th} International Conference on Fluid Sealing, B.H.R.A., Paper K1, pp. 698-709, 1987.

[3] Salant, R.F., *Numerical Analysis of the Flow Field Within Lip Seals Containing Microundulations*, ASME Journal of Tribology, Vol. 114, pp. 485-492, 1992.

[4] Stakenborg, M.J.L., *On the Sealing Mechanism of Radial Lip Seals*, Tribology International, Vol. 21, pp. 335-340, 1988.

[5] Stakenborg, M.J.L., van Leeuwen, H.J. and ten Hagen E.A.M., *Visco-Elastohydrodynamic (VEHD) Lubrication in Radial Lip Seals: Part I - Steady-State Dynamic Viscoelastic Seal Behavior*, ASME Journal of Tribology, Vol. 112, pp. 578-583, 1990.

[6] van Leeuwen, H.J., and Stakenborg M.J.L., *Visco-Elastohydrodynamic (VEHD) Lubrication in Radial Lip Seals: Part 2 - Fluid Film Formation*, ASME Journal of Tribology, Vol. 112, pp. 584-592, 1990.

[7] G. Colombo ed E. Prati, *Condizioni di Tenuta con Guarnizioni Radiali per Alberi Rotanti*, atti del XV Congresso AIMETA di Meccanica Teorica e Applicata, 26-28 Settembre, Taormina, 2001. Sommario pag. SP ME 20.

[8] M. Amabili, G. Colombo and E. Prati, *Leakage of Radial Lip Seals at Large Dynamic Eccentricities*, Proceedings of the 16^{th} International Conference on Fluid Sealing, 18-20 September 2000, Brugge, Belgium, pp. 321-333.

[9] M. Amabili, G. Colombo and E. Prati, *On the Leakage of Radial Lip Seals*, Proceedings of 2000 AIMETA International Tribology Conference, 20-22 September, L'Aquila, Italy, pp. 565-572

[10] Amabili M., Colombo G., Prati E., *Impiego della FRF nella Caratterizzazione di Anelli di Tenuta in Elastomero*, V Convegno AIMETA di Tribologia, Varenna (Lc) 1998; pp. 191-202.

[11] Chung Kyun Kim, Woo Jeon Shim, *Analysis of Contact Force and Thermal Behaviour of Lip Seals*, Tribology International, Vol. 30, N° 2, pp. 113-119, 1996.

[12] Vionet C.A., *Numerical Investigation of the Sealing Capacity of Centrifugal Instabilities in Shaft Seals*, Int. J. Heat and Flow, Vol. 16, N° 4, August 1995.

[13] W. Flugge, Viscoelasticity, Springer-Verlag, Berlin 1975.

[14] Stakenborg M.J.L., Van Ostayen R.A.J., *Radial Lip Seals, Thermal aspects*, Proceedings of the 15^{th} Tribological Design of Machine Elements, Leeds 1989, Ed. Elsevier, Amsterdam, ISBN 0-444-874356, pp. 79-88.

[15] M. Amabili, G. Colombo and E. Prati, *Experiments on the Dynamics of a Rubber Ring Seal*, Proceedings of the 17^{th} International Modal Analysis Conference (IMAC), February 8-11, 1999, Orlando, USA, pp. 297-301.

[16] T. Kanaya, H. Inoue, Y. Shimotsuma, *Study of lip behaviour in rotary oil seals*, 10^{th} International Conference on Fluid Sealing, Innsbruck, Austria 1984, pp. 439-449.